Excitation-energy-dependent potential energy surfaces in the ternary breakup of ^{252}Cf

C. Karthikraj[1,*] and Zhongzhou Ren[1,2,†]

[1]*School of Physics Science and Engineering, Tongji University, Shanghai – 200092, China*

[2]*Key Laboratory of Advanced Micro-Structure Materials, Ministry of Education, Shanghai – 200092, China*

(Received 23 January 2019; revised manuscript received 15 November 2019; published 7 January 2020)

We study the excitation energy-dependent potential-energy surfaces (PESs) for both the spherical and deformed fragments from the ternary fragmentation (TF) of ^{252}Cf at four different excitation energies of the fissioning parent nuclei. A two-dimensional minimization approach with respect to the charge numbers (Z_1, Z_2, and Z_3) of the fragments has been used to minimize all possible ternary combinations, which are generated from the atomic-mass-evaluation (AME2016) data [Chin. Phys. C **41**, 030003 (2017)]. To calculate the energy-dependent TF-PES, we used the temperature-dependent binding energies (TDBE), which are calculated as follows: the temperature-dependent (T-dependent) macroscopic liquid-drop model (LDM) energy proper due to Krappe's formula [Phys. Rev. C **59**, 2640 (1999)] and the microscopic shell correction energies due to the analytical estimates of Myers and Swiatecki [Nucl. Phys. **81**, 1 (1966)]. Furthermore, the shell correction energies and the nuclear deformations are also made T-dependent. In this study, the T-dependent total interaction potential between the ternary fragments is calculated for the fragments in a collinear geometry with the lightest fragment A_3 being in the middle of the two main fission fragments A_1 and A_2. From the TF-PES results with the use of spherical-shell corrections, a strong energy maximum in the PES is obtained around $Z_3 = 2$ with the $Z_1 = 50$ region due to the closed-shell effects of doubly magic nuclei. In addition to this, we also obtained some other significant energy maxima around the magic and/or semimagic numbers of nuclei. These energy maxima extend further with increasing excitation energy of the fissioning parent nuclei. We also found that the true-ternary-fragmentation (TTF) fragments are reasonably favored at high excitation energies. Furthermore, the effects of T-dependent deformations and the T-dependent deformed-shell corrections in the TF-PES of ^{252}Cf are also studied. From the TF-PES results of deformed ternary fragments, we obtained the energy maximum around $Z_3 = 16$ region, which may be due to the larger β_2 deformation values. Furthermore, we also studied the ternary fragmentation yields and neutron emission from the excited fragments in the ^{10}Be-accompanied spontaneous ternary fission of ^{252}Cf and compared our calculated results with the available experimental data.

DOI: 10.1103/PhysRevC.101.014603

I. INTRODUCTION

Since the discovery of nuclear fission [1] in 1938, a lot of theoretical and experimental investigations have been performed to study the fission process. However, fission physics still has interesting topics to be explored and understood. One of them is the very rare process of nuclear ternary fission, which is the breakup of a heavy compound nucleus into three fragments. It is well known that the possibility of exotic ternary decay is much less than for binary decays, which was recently reported [2] as $\approx 4 \times 10^{-3}$ per spontaneous fission event. Generally, the ternary fission process can happen in either direct (equatorial and collinear) or cascade fission modes. The term "ternary fission" is often referred to as the light-charged-particle–accompanied (LCP-accompanied) fission because the emitted third fragment is very light and, in most cases, is an α particle with the largest probability in the perpendicular direction to the binary fission axis (equatorial configuration). However, LCP-accompanied fission gives decreasing yields as a function of increasing the mass of the third particle. Another term "true-ternary-fission" refers to the spontaneous breakup of a heavy nucleus into three collinear fragments of comparable masses. Recent experimental observation [2,3] and numerous theoretical predictions [4–6] suggest that, in a ternary decay, the collinear configuration is comparatively favored over the equatorial configuration.

Lestone [7,8] proposed an evaporation-based model for nuclear ternary fission, which is a blend of statistical [9] and dynamical [10] models of nuclear fission. Using this hybrid model, ternary fission probabilities for thermal-neutron-induced fission of ^{242}Pu(n_{th}, f) were calculated and the results agree very well with the experimental results of Koster *et al.* [11]. Andreev *et al.* [12] studied the different LCP (^{4}He, ^{10}Be, ^{14}C, and ^{20}O) accompanied ternary fission of ^{252}Cf within the statistical approach of two-step binary process. They also calculated the charge distributions in spontaneous ternary fission of ^{252}Cf and in induced ternary fission of ^{56}Ni and obtained a good comparison with the available experimental data. Pyatkov *et al.* [2,3] experimentally observed the true-ternary-fragmentation (TTF) in thermal-neutron-induced

*c.karthikraaj@gmail.com

†zren@tongji.edu.cn

 ©2020 American Physical Society

fission of ^{235}U(n$_{th}$, f) and in spontaneous fission (sf) of ^{252}Cf with the use of the missing-mass technique. The authors called this process "collinear cluster tripartition" (CCT), in which three fragments with proton magic numbers $Z_1 = 50$, $Z_2 = 28$, and $Z_3 = 20$ have been observed. Furthermore, within the concept of the dinuclear system (DNS) model, the PES for the CCT products from the ternary fission of ^{235}U(n$_{th}$, f) and ^{252}Cf(sf) is studied in Refs. [13–16].

Using the two-center shell model (TCSM), Zagrebaev *et al.* [17,18] studied the PES for the superheavy nucleus $^{296}_{116}$X formed in the collision of ^{48}Ca with ^{248}Cm and found that the TTF with the formation of a heavy third fragment is possible for superheavy nuclei. In addition, they also studied the ternary fission PES of giant nuclear systems $^{466,476}_{184}$X formed in $^{233,238}_{92}$U + $^{233,238}_{92}$U low-energy collisions and reported that the PES has a deep minimum for Pb + Ca + Pb and Hg + Cr + Hg ternary configurations apart from the Pb + No binary configuration. Karpov [19] developed the three-center shell model (T3CSM) for a deformed nucleus to study the potential-energy landscape for the ternary fission of ^{252}Cf and reported that the favorable pronounced valleys for the ternary fission mode consists of doubly magic Sn (with $Z = 50$ and $N = 82$) as one of the fragments and two other magic and/or semimagic fragments. Recently, Denisov *et al.* [20] studied the total interaction potential energies of various deformed fragments formed in the ternary fission of ^{252}Cf and compared their calculated ternary particles yield with the available experimental data [21] for the ternary fission reaction of ^{249}Cf(n$_{th}$, f).

Within the three-cluster model (TCM) proposed by Balasubramaniam *et al.* [6,22–27], TF-PES for two different arrangements of ternary fragments, *viz.* keeping the lightest fragment A_3 in the middle (type 1) and keeping a lighter fragment A_2 in the middle (type 2), in the collinear ternary fission of ^{252}Cf are discussed [26] and they reported the various possible energetically favored ternary fission modes. Santhosh *et al.* [28–30], studied the β_2 deformation effects in the α-accompanied ternary fission of even-even $^{238–244}$Pu, $^{244–252}$Cm, and $^{244–260}$Cf nuclei, using the unified ternary fission model. Based on the framework of the statistical theory of fission, one of us (C.K.) [31] studied the ternary fragmentation mass distribution of ^{252}Cf for $A_3 = {}^{48}$Ca at $T = 1$ and 2 MeV and obtained the largest yield for the experimental expectation of ^{132}Sn + ^{72}Ni + ^{48}Ca ternary fragmentation. It is to be noted here that the authors have considered these temperature values as the temperature of the fission fragments. Furthermore, they have not considered the T-dependence of the fission fragments deformation. In Ref. [32], we further extended this approach to study the mass and charge distributions of different LCP-accompanied fission of ^{252}Cf with $A_3 = {}^4$He, ^{10}Be, ^{14}C, ^{20}O, ^{20}Ne, and ^{24}Ne and the obtained yield values are in good agreement with the available experimental data.

The present paper aims to extend our previous work carried out in Ref. [35] by introducing the excitation-energy dependence of the PES in the ternary fragmentation of ^{252}Cf. For the calculation of temperature-dependent binding energies, we have used the T-dependent liquid-drop model (LDM) energy proper due to Krappe's formula [33]. In Krappe's formula, the Yukawa-plus-exponential mass formula is generalized to describe the Gibbs free energy of hot and finite nuclei. Furthermore, the T dependence of the main liquid drop coefficients is obtained by fitting the results of the T-dependent Thomas Fermi calculations. One of us (C.K.) [36,37] has already studied the effects of Krappe's T-dependent formula in the binary decay of excited ^{56}Ni* and ^{59}Cu* nuclei. It is concluded from these studies [36,37] that the refitting of the coefficients of the Krappe's T-dependent binding-energy formula is not necessary and the structural effects on the PES is the intrinsic property of the binding-energy form one uses. Hence, we have used here the actual form of the expression given in Ref. [33] to calculate the T-dependent LDM energy. Besides Krappe's macroscopic LDM energy, the microscopic shell corrections due to the analytical estimates of Myers and Swiatecki [38] are also added to reproduce the ground-state experimental binding energies. The difference between the calculated ground-state binding energies due to Krappe's formula and the experimental ground-state binding energies from the AME2016 data [34] is presented in Fig. 1 for the experimentally known 3436 nuclei. From this figure, it is seen that the binding energies calculated with the use of Krappe's formula has less deviation (except at the vicinity of the magic nuclei, where the difference is noted around 5 MeV) with respect to the experimental data for the nuclei of interest (nuclei presented under the dotted lines). Furthermore, we can also see that the deviations for light nuclei are slightly larger than those for heavy nuclei, which may be due to the shortage of LDM in describing the significant structural effects of the light nuclei. It is to be mentioned that the difference between the calculated and the experimental binding energies [39] is already shown for the selective isobars with $A = 12$, 56, 82, and 116 in Ref. [36].

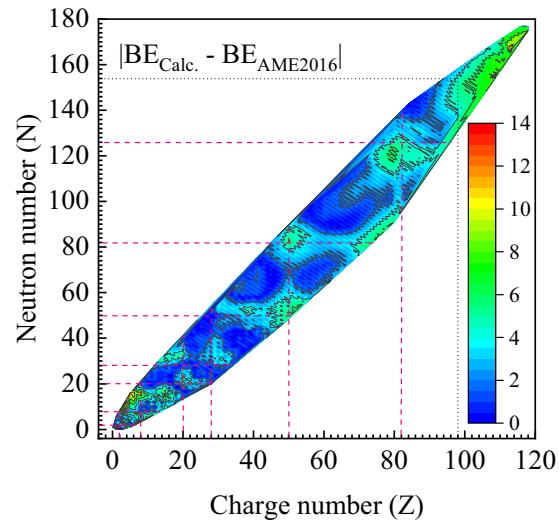

FIG. 1. The difference between the calculated ground-state binding energies with the use of the Krappe formula [33] and the experimental ground-state binding energies from the AME2016 data [34] is presented for the experimentally known 3436 nuclei. The horizontal and vertical dotted lines correspond to the neutron ($N = 154$) and proton ($Z = 98$) numbers of $^{252}_{98}$Cf nuclei, respectively. The dashed lines correspond to the magic numbers of proton and neutron.

The organization of the paper is as follows: A brief description of the theoretical framework used in our calculations is given in Sec. II. The calculations and results are discussed in Sec. III. Finally, the summary of our results and conclusions are given in Sec. IV.

II. THEORETICAL FRAMEWORK

The ternary fragmentation is energetically possible only if the Q value of the reaction is positive,

$$Q = \sum_{i=1}^{3} \mathrm{BE}_i(T_\ell) - \mathrm{BE}_f > 0. \tag{1}$$

Here $\mathrm{BE}_i(T_\ell)$ ($i = 1$, 2, and 3) and BE_f are the T-dependent binding energies (in MeV) of the three fission fragments and the ground-state binding energy of the fissioning nucleus ^{252}Cf, respectively, and T_ℓ is the temperature value of the ternary system, to be defined later. It is to be mentioned here that the energy dependence of the fissioning nucleus enters through its excitation energy ξ_f^* only. The T-dependent binding energies are calculated as

$$\mathrm{BE}(T) = \mathrm{LDM}(T) + \delta U \exp\left(-T^2/T_0^2\right), \tag{2}$$

where the macroscopic term $\mathrm{LDM}(T)$ is the T-dependent liquid-drop energy proper due to Krappe's form [33] and δU is the microscopic shell corrections due to the analytical estimates of Myers and Swiatecki [38], also made T dependent to vanish exponentially with $T_0 = 1.5$ MeV.

In this framework, the T-dependent total interaction potential between the three touching fragments in type-1 collinear geometry (for the details of this geometry, refer to Fig. 1 in Ref. [35]) is the sum of the pairwise Coulomb and nuclear interaction potentials between fragments and deformation energies of the three fission fragments, which can be written as

$$V = \sum_{i=1}^{3}\sum_{j>i}^{3} V_{ij}^{\mathrm{C}}[R_{ij},\ \beta_{\lambda i}(T_\ell),\ \beta_{\lambda j}(T_\ell)] + V_{ij}^{\mathrm{N}}[R_{ij},\ \beta_{\lambda i}(T_\ell),\ \beta_{\lambda j}(T_\ell)] + \sum_{i=1}^{3} E_i^{\mathrm{def}}[\beta_{\lambda i}(T_\ell)], \tag{3}$$

where V_{ij}^{C} and V_{ij}^{N} corresponds to the T-dependent Coulomb and nuclear interaction potentials between fragments i and j, respectively, and $E_i^{\mathrm{def}}[\beta_{\lambda i}(T_\ell)]$ is the T-dependent deformation energy of fragment i. In Eq. (3), one can also include the centrifugal-potential term. However, a recent study [25] reported that the inclusion of centrifugal potential does not significantly vary the structure of the potential and its role is restricted only to shifting the potential up. Hence, we do not consider this term in the present study.

It is to be noted that the ground-state static deformation values $\beta_{\lambda i}$ ($\lambda = 2$, 3, 4, and 6) of the finite-range droplet model-2012 (FRDM2012) [40] was used in Ref. [35]. However, in order to obtain the fully energy- and/or T-dependent TF-PES, the T-dependence of the deformation values $\beta_{\lambda i}(T)$ calculated as in Refs. [41–43] are considered through the following relation:

$$\beta_{\lambda i}(T) = \beta_{\lambda i}^{\mathrm{g.s.}} \exp(-T/T_0), \tag{4}$$

where $\beta_{\lambda i}^{\mathrm{g.s.}}$ is the ground-state deformation values and T_0 is the temperature of the nucleus at which the shell effects start to vanish ($T_0 = 1.5$ MeV).

The surface radius of a deformed nucleus is defined as the distance from the origin of the coordinate system to the point on the nuclear surface whose position is specified by the orientation angles,

$$R_i(\theta_i, T_\ell) = R_{0i}(T_\ell)\left[1 + \sum_{\lambda} \beta_{\lambda i}(T_\ell) Y_\lambda^{(0)}(\theta_i)\right], \tag{5}$$

where $R_{0i}(T_\ell)$ is the T-dependent nuclear radii of the equivalent spherical nuclei, which can be written as

$$R_{0i}(T_\ell) = \left(1.2536A_i^{1/3} - 0.80012A_i^{-1/3} - 0.0021444/A_i\right) \times \left[1 + \left(7.62 \times 10^{-4} T_\ell^2\right)\right], \tag{6}$$

where $Y_\lambda^{(0)}$ is the spherical harmonic function and θ_i is the angle between the symmetry axis and the radius vector $R_i(\theta_i)$ of the nuclei. In this study, the orientation angles are considered to be 0°. The first term presented in Eq. (6) is obtained from Ref. [44] and its T dependence is taken from Ref. [33].

The Coulomb interaction energy V_{ij}^{C} defines the force of repulsion between the two interacting charges of fragments, i and j. The expression of the Coulomb interaction of the two deformed arbitrarily oriented axial-symmetric nuclei [45] is rewritten in Ref. [35] by taking into consideration higher-order deformations as well as the 0° orientation angle, and its T dependence is given by

$$\begin{aligned} &V_{ij}^{\mathrm{C}}[R_{ij}, \beta_{\lambda i}(T_\ell), \beta_{\lambda j}(T_\ell)] \\ &= \frac{Z_i Z_j e^2}{R_{ij}}\left\{1 + \frac{3\left[R_{0i}^2(T_\ell)\beta_{2i}(T_\ell) + R_{0j}^2(T_\ell)\beta_{2j}(T_\ell)\right]}{2\sqrt{5\pi}R_{ij}^2} + \frac{3\left[R_{0i}^3(T_\ell)\beta_{3i}(T_\ell) + R_{0j}^3(T_\ell)\beta_{3j}(T_\ell)\right]}{2\sqrt{7\pi}R_{ij}^3}\right. \\ &+ \frac{\left[R_{0i}^4(T_\ell)\beta_{4i}(T_\ell) + R_{0j}^4(T_\ell)\beta_{4j}(T_\ell)\right]}{2\sqrt{\pi}R_{ij}^4} + \frac{3\left[R_{0i}^6(T_\ell)\beta_{6i}(T_\ell) + R_{0j}^6(T_\ell)\beta_{6j}(T_\ell)\right]}{2\sqrt{13\pi}R_{ij}^6} \\ &\left. + \frac{3\left[R_{0i}^2(T_\ell)\beta_{2i}^2(T_\ell) + R_{0j}^2(T_\ell)\beta_{2j}^2(T_\ell)\right]}{7\pi R_{ij}^2} + \frac{9\left[R_{0i}^4(T_\ell)\beta_{2i}^2(T_\ell) + R_{0j}^4(T_\ell)\beta_{2j}^2(T_\ell)\right]}{14\pi R_{ij}^4} + \frac{27R_{0i}^2(T_\ell)\beta_{2i}(T_\ell)R_{0j}^2(T_\ell)\beta_{2j}(T_\ell)}{10\pi R_{ij}^4}\right\}, \end{aligned} \tag{7}$$

where $e^2 = 1.44$ MeV fm, Z_i and Z_j are, respectively, the number of protons in nuclei i and j, and R_{ij} is the distance between the mass centers of nuclei i and j: $R_{ij} = R_i(\theta_i, T_\ell) + R_j(\theta_j, T_\ell)$ fm.

The T-dependent nuclear interaction potential $V_{ij}^{\rm N}$ between two deformed nuclei [20] can be written as

$$V_{ij}^{\rm N}[R_{ij},\ \beta_{\lambda i}(T_\ell),\ \beta_{\lambda j}(T_\ell)] \approx S[\beta_{\lambda i}(T_\ell),\ \beta_{\lambda j}(T_\ell)]V_{0ij}^{\rm N}\{d_{0ij}[R_{ij}^{\rm sph},\ R_{0i}(T_\ell),\ R_{0j}(T_\ell)]\}. \tag{8}$$

Here $S[\beta_{\lambda i}(T_\ell),\ \beta_{\lambda j}(T_\ell)]$ relates to the modification of the strength of nuclear interaction of the deformed nuclei induced by the surface deformations, which depends on the mean curvature of nuclear surfaces at the closest points and is given by

$$S[\beta_{\lambda i}(T_\ell),\ \beta_{\lambda j}(T_\ell)] = \frac{\frac{R_i^2(\pi/2,T_\ell)R_j^2(\pi/2,T_\ell)}{R_i^2(\pi/2,T_\ell)R_j(0,T_\ell)+R_j^2(\pi/2,T_\ell)R_i(0,T_\ell)}}{\frac{R_{0i}(T_\ell)R_{0j}(T_\ell)}{R_{0i}(T_\ell)+R_{0j}(T_\ell)}}.$$

The factor $S = 1$, $S < 1$, and $S > 1$ corresponds to both spherical, both prolate deformed, and both oblate deformed interacting nuclei, respectively. The second term in Eq. (8) represents the nuclear part of the interaction potential between the same nuclei, but with spherical shape [44], and is defined as

$$V_{0ij}^{\rm N}\{d_{0ij}[R_{ij}^{\rm sph},\ R_{0i}(T_\ell),\ R_{0j}(T_\ell)]\} = \frac{\nu_1 C + \nu_2 C^{1/2}}{1 + \exp\left(\frac{d_{0ij}}{d_1 + d_2/C}\right)},$$

where $\nu_1 = -27.190$ MeV fm^{-1}, $\nu_2 = -0.93009$ MeV fm$^{-1/2}$, $d_1 = 0.78122$ fm, $d_2 = -0.20535$ fm^2, $C = \frac{R_{0i}(T_\ell)R_{0j}(T_\ell)}{R_{0i}(T_\ell)+R_{0j}(T_\ell)}$ fm, and $R_{ij}^{\rm sph} = R_{0i}(T_\ell) + R_{0j}(T_\ell)$ fm. Here d_{0ij} is the closest distance between the surfaces of two interacting nuclei, and it is taken as zero for the collinear touching fragments. The nuclear interaction between fragments A_1 and A_2 is not considered here, because of the short-range nuclear interaction.

Furthermore, the deformation energy of the fission fragment consists of the surface and Coulomb contributions caused by deviation from spherical shape [46,47] and is

$$E_i^{\rm def}[\beta_{\lambda i}(T_\ell)] = \sum_\lambda \left[\frac{(\lambda-1)(\lambda+2)b_{\rm surf}A_i^{2/3}}{4\pi} - \frac{3(\lambda-1)e^2Z_i^2}{2\pi(2\lambda+1)R_{0i}(T_\ell)}\right]\frac{\beta_{\lambda i}^2(T_\ell)}{2}, \tag{9}$$

where $b_{\rm surf}$ is the surface energy coefficient of the mass formula taken from Ref. [40].

The total excitation energy (E^*) of three fission fragments is related to the Q value as follows:

$$E^* = \xi_f^* + Q - V. \tag{10}$$

Here ξ_f^* is the excitation energy of the fissioning parent nucleus and V is the total interaction potential between the three interacting fragments. To see the variation of TF-PES as a function of excitation energy and/or temperature, we consider here four different excitation energies of the fissioning parent nucleus, i.e., $\xi_f^* = 0$ MeV (for spontaneous fission), 6.17 MeV (for thermal-neutron-induced fission), 25 MeV, and 50 MeV.

Generally, in binary-fission studies, the total excitation energy is assumed to be distributed between the two fission fragments proportional to their masses or level-density parameters. The same assumption is extended here for ternary fission fragments and it is given by

$$\mathcal{E}_i^* = \frac{E^* a_i}{a_1 + a_2 + a_3}. \tag{11}$$

The above assumption was already applied by Denisov *et al.* [20] for the yield calculation of various ternary fragments in the fission of ^{252}Cf. It is to be noted that Eq. (11) is different from Eq. (12) of Ref. [12], where the excitation energy of the third fragment is assumed to be small. However, in this study, it is calculated as that of the primary fragments by using Eq. (11).

The level-density parameter a_i [12,48] is calculated as

$$a_i = \tilde{a}_i(A_i)\left[1 + \frac{1 - \exp(-E^*/E_D)}{E^*}\delta U_i\right]. \tag{12}$$

Here $\tilde{a}_i(A_i) = 0.114A_i + 0.098A_i^{2/3}$ MeV^{-1} [49] and the damping constant $E_D = 18.5$ MeV. The temperature value of the ternary system is calculated as, $T_\ell = \sqrt{\mathcal{E}_i^*/a_i}$. The T_ℓ value is the same for all three fragments in a particular ternary decay but varies for different ternary decay with the various mass and charge combinations of the ternary fragments. Since the binding energies BE$_i$ of the ternary fragments and the total interaction potential V between them depend on the temperature T_ℓ of the corresponding ternary system, the total excitation energy E^* is calculated with Eq. (10) by using an iteration procedure: i.e., first, the ternary fragments binding energies and the total interaction potentials are calculated with $T = 0$ MeV and a new value of E^* is obtained from Eq. (10). Then, with this E^*, we calculate the T_ℓ value of each ternary system. For each ternary system with its corresponding T_ℓ, we calculate Q and V which leads to a new value of E^*. A similar approach is already done in Refs. [12,50] and reported that a nice accuracy was obtained in finding E^*.

In Ref. [31], the ternary fragmentation probability is considered to be proportional to the product of nuclear level densities (ρ) of three fission fragments,

$$P(A_j, Z_j) \propto \prod_{i=1}^{3} \rho_i. \tag{13}$$

The nuclear level density ρ_i at an excitation energy $\mathcal{E}_i^*$ is given by

$$\rho_i(\mathcal{E}_i^*) = \frac{\sqrt{\pi}}{12}\frac{\exp(2\sqrt{a_i\mathcal{E}_i^*})}{a_i^{1/4}\mathcal{E}_i^{*5/4}}. \tag{14}$$

The neutron emission from the excited fission fragments can be calculated as in Ref. [12],

$$\nu_i = \mathcal{E}_i^*/\left(S_n^i + 2T_\ell\right), \tag{15}$$

where S_n^i is the separation energy of the neutron in the fragment i, calculated as the ground-state binding-energy difference between the fragments (A_i, Z_i) and $(A_i - 1, Z_i)$.

III. RESULTS AND DISCUSSION

In this study, one of the important features is the use of T-dependent binding energies due to Krappe's formula. This formula has already been successfully applied in the dynamical cluster-decay model (DCM) by one of us (C.K.) [36,37] for the calculation of binary fragmentation potential energies of ^{56}Ni* and ^{59}Cu* nuclei at different temperatures. The detailed description of the DCM can be found in Ref. [51]. Here, we extended the works carried out in Refs. [35–37] to analyze the excitation-energy dependence of the potential-energy surfaces for the ternary fragmentation of ^{252}Cf.

A. Calculation of total excitation energy E^*

At first, all possible ternary fragment combinations for the ternary fragmentation of ^{252}Cf are generated with the use of AME2016 data by imposing the conditions such that always, $A_1 + A_2 + A_3 = A_F$ and $Z_1 + Z_2 + Z_3 = Z_F$ (to conserve the mass and charge numbers in a ternary fission reaction), and $A_1 \geqslant A_2 \geqslant A_3$ and $Z_1 \geqslant Z_2 \geqslant Z_3$ (to avoid the repetition of fragment combinations). Here, A_F, A_1, A_2, and A_3 and Z_F, Z_1, Z_2, and Z_3 correspond to the mass and charge numbers of the fissioning parent nucleus and the three fission fragments, respectively. Furthermore, A_1 and A_3 are denoted as the heaviest and the lightest of the three fragments, respectively. For all possible thus-generated ternary fragment combinations, the macroscopic liquid-drop energy proper due to Krappe's formula [33], microscopic shell correction energies due to the analytical estimates of Myers and Swiatecki [38], and the total interaction potential between the three fragments are calculated with the use of the theoretical formalism presented in Sec. II. In the present study, the calculations are carried out for four different excitation energies of the fissioning parent nucleus considered. As mentioned in the earlier section, the binding energies of the ternary fragments and the total interaction potential between them depend on the excitation energy and/or temperature. Hence, for each ξ_f^*, the total excitation energy E^* of every possible ternary fragmentation is calculated by using an iteration procedure; *viz.* first, the ternary fragments binding energies and the total interaction potentials are calculated with $T = 0$ MeV by using Eqs. (2) and (3), respectively, and a new value of E^* is found from Eq. (10). Then, with this E^*, we calculate the temperature T_ℓ value of each ternary fragmentation with the use of Eqs. (11) and (12). Finally, for each ternary fragmentation with its corresponding T_ℓ, we calculate the ternary fragments T-dependent binding energies and T-dependent total interaction potential which leads to a new value of E^*. In this study, the ternary fragmentation potential-energy surface in terms of the total excitation energy of the three fission fragments is considered. Furthermore, for the minimization of all possible ternary fragment combinations on the potential-energy surface we have used the same two-dimensional approach as done in our earlier work [35] but for the charge numbers (Z_1, Z_2, and Z_3) of the three fission fragments. The ternary fragment combination with the highest value of E^* is considered to be the most favorable ternary fragment configuration. It is to be mentioned here that in Ref. [35], we presented $V - Q$ as the driving potential and reported the smallest driving potential as a favorable region. However, we present here $\xi_f^* + Q - V$ as the ternary fragmentation PES. Hence we focus the maximum PES to identify the favorable ternary configuration.

It is important to mention that, in Ref. [52], the authors studied the charge distribution in the ternary fragmentation of ^{252}Cf at four different excitation energies of the parent nucleus. Furthermore, the total excitation energy of the fragments involved in each ternary fragmentation was kept the same as that of the excitation energy of the parent nucleus. This has been achieved by the iterative computation of temperature values of the fragments presented in each ternary fragmentation. However, in the present study, the total excitation energy of the fragments has derived from the energy conservation [as defined in Eq. (10)] in a ternary fission reaction, and it is found varying as a function of mass and charge numbers of the three fragments. Consequently, the PES has different temperature values as a function of mass and charge numbers of the three fragments.

B. Effect of spherical-shell corrections on the ternary fragmentation potential-energy surface

We now discuss the effect of spherical-shell corrections on the T-dependent potential-energy surfaces for the ternary fragmentation of ^{252}Cf at different excitation energies of the fissioning parent nucleus. Here the fragments are considered to be spherical and the shell corrections are also made T dependent. With the use of the theoretical formalism presented in Sec. II, we calculate the binding energies and the total interaction potentials of every possible ternary combination. By using an iterative process as discussed earlier, we calculate the excitation energies for all possible ternary fragment combinations. The influence of T-dependent spherical-shell corrections on the TF-PES of two-dimensional proton minimized ternary fragment combinations are presented in the ternary plots of Fig. 2. Figures 2(a)–2(d) correspond to the four different excitation energies of the fissioning parent nucleus. Here the proton magic numbers are shown as dashed lines to see the importance of spherical-shell correction energies due to the closed-shell effects. The number of ternary fragment combinations (which have $E^* > 0$) presented in each panel increases with the increase of ξ_f^*. For the spontaneous fission of ^{252}Cf, the ternary charge combinations Cd + Ge + Ar, Sn + Zn + Ar, Te + Zn + S, and Sn + Ni + Ca also possesses larger excitation energy and reasonably favored. This is in line with the experimental observation. Furthermore, for $\xi_f^* = 0$ MeV, the occurrence of heavier third fragments is less probable and it is experimentally known. However, from $\xi_f^* \geqslant 25$ MeV, a region of TTF fragments with larger excitation energy is also obtained. In other words, the occurrence of heavier third fragments increases with rising ξ_f^*. Irrespective of the ξ_f^* considered, the largest excitation energy maximum in the PES is seen around $Z_3 = 2$–4 with $Z_2 = 40$–48 and $Z_1 = 48$–54 region due to the closed-shell effects of the doubly magic numbers of nuclei, $^4_2$He and $^{132}_{50}$Sn. Interestingly, this energy maximum increases further with the increase in ξ_f^*. Besides this energy maximum, some other notable energy maxima are also found around $Z_3 = 12$–14 with

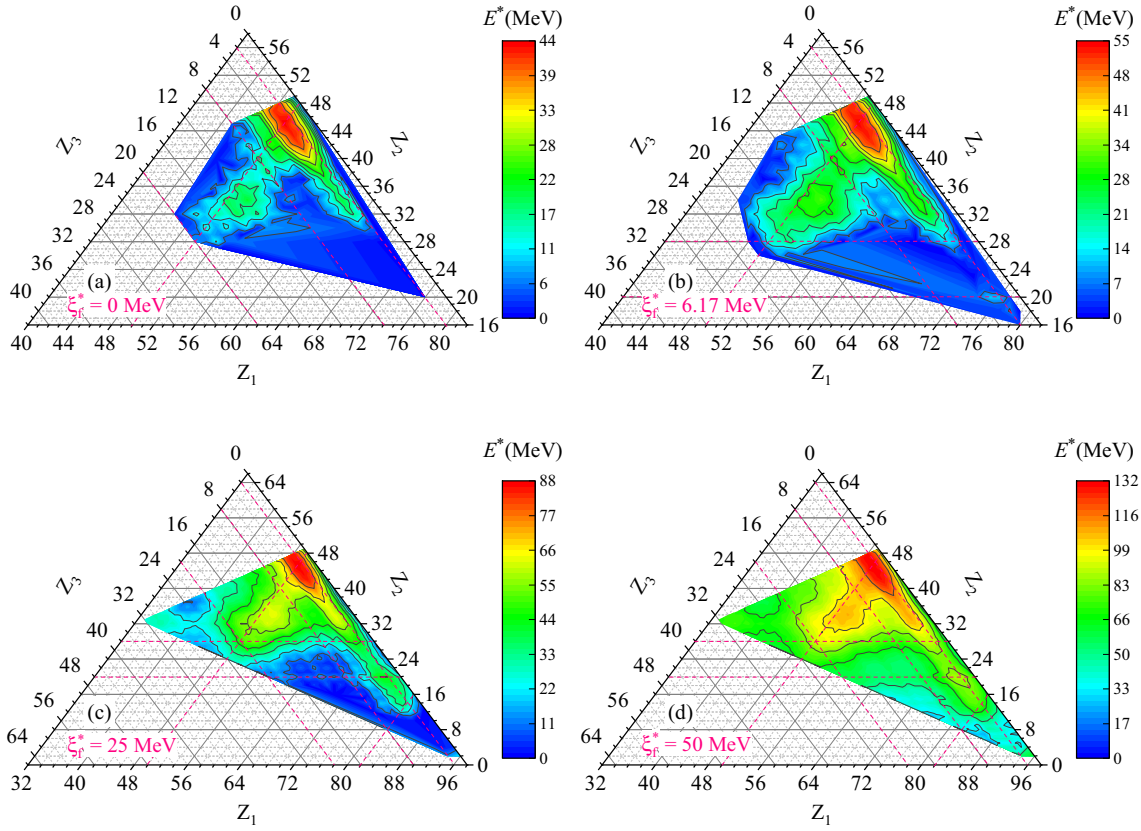

FIG. 2. T-dependent PES of proton minimized spherical collinear touching fragments from the ternary fragmentation of ^{252}Cf nuclei. Panels (a)–(d) correspond to the different excitation energies of the fissioning parent nuclei, such as $\xi_f^* = 0$ (sf), 6.17 (n_{th}, f), 25, and 50 MeV, respectively. The dashed lines correspond to the proton magic numbers.

$Z_2 = 32$–36 and $Z_1 = 50$–52, $Z_3 = 8$ with $Z_1 = 50$–52, and $Z_2 = 20$ with $Z_3 = 2$ region, due to the closed-shell effects of the magic and/or semimagic numbers of nuclei. In the manner of the largest-energy maximum found around $Z_3 = 2$–4, these maxima are also increasing further with the increase of ξ_f^*. Due to the variation of T_ℓ for each ternary fragmentation, the vanishing of shell structures at higher excitation energies is not noticeable.

C. Effect of deformed-shell corrections on the ternary fragmentation potential-energy surface

The effect of T-dependent deformations and the T-dependent deformed-shell corrections on the TF-PES of ^{252}Cf is presented in the ternary plots of Fig. 3. Figures 3(a)–3(d) correspond to the four different excitation energies of the fissioning parent nucleus, respectively. The calculation procedure for the total excitation energy E^* of deformed ternary fragments is similar to the spherical ternary fragments, except that the fragment-deformation effects are also considered instead of the spherical fragments. Furthermore, the shell correction energies made dependence on the deformation as well as the temperature. For the spontaneous fission studies, the ground-state deformations are taken from the FRDM2012 [40] data, and for other excitation energies, the T-dependent deformation energies of the fragments are considered through Eq. (4). It is to be noted that the deformation values are considered for $A \geqslant 16$ and $Z \geqslant 8$ nuclei and not for lighter systems with $A < 16$ and $Z < 8$. Furthermore, the inclusion of β_2 deformation is sufficient since it has a larger effect on the PES than the other higher-order (β_3, β_4, and β_6) deformations [35]. To maintain consistency with our earlier work [35], we considered here all higher-order deformations as well. In Fig. 3, a strong energy maximum in the TF-PES is found around $Z_3 = 16$ with $Z_2 = 38$–34 and $Z_1 = 44$–48 region. It is worth to be mentioned that the ternary fragments presented in this region have larger β_2 deformation values, particularly for $Z_3 = 16$. Because of this larger β_2 deformations, the total interaction potential energy of these ternary fragments got reduced, and hence it has a larger total excitation energy. Furthermore, a strong maximum also appears around $Z_3 = 2$–4 with $Z_2 = 42$–48 and $Z_1 = 48$–52 region with increasing excitation energy of the fissioning nucleus. From $\xi_f^* \geqslant 25$ MeV, apart from true-ternary-fragmentation region, $Z_3 = 8$ with $Z_2 = 44$ and $Z_1 = 46$, and $Z_2 = 20$ with $Z_3 = 2$ region fragments also possesses larger excitation energy.

D. Ternary fragmentation yields and neutron emission

Based on the experimental [53] and theoretical [23,32,54] investigations, we have studied the ternary fragmentation yields for the spontaneous ternary fission of ^{252}Cf with ^{10}Be as the third fragment. Since the third fragment is fixed

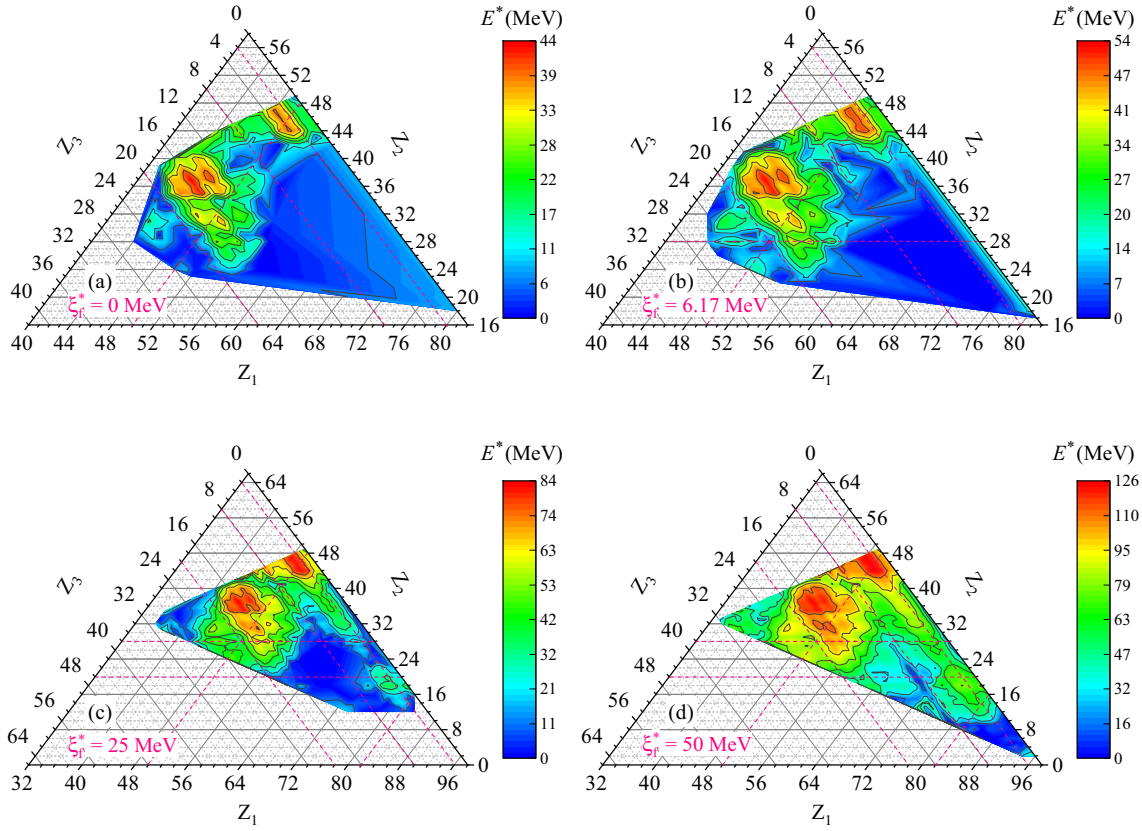

FIG. 3. Same as Fig. 2 but for the deformed collinear touching ternary fragments with the use of T-dependent deformations and the T-dependent deformed-shell correction energies.

with $A_3 = 10$ and $Z_3 = 4$, the other two fragments' mass and charge numbers (A_1, Z_1 and A_2, Z_2) are obtained by satisfying the conservation of mass and charge numbers of the fissioning nucleus and the three fission fragments, respectively. Here the fragments are assumed to be spherical. For these obtained ternary fragment combinations, the ternary fragmentation yields are calculated by normalizing the ternary fragmentation probability to 200%, which is the production yield of the other two main fragments for a fixed third fragment ^{10}Be. In Fig. 4, we present the comparison of our calculated ternary fragmentation yield results (open circles) for the ^{10}Be-accompanied spontaneous ternary fission of ^{252}Cf with the available experimental data (solid circles) [53] of the measured fragmentation channels. From this figure, it is seen that our calculated yields are comparable with the experimental data for the following fragmentation channels: ^{102}Zr + ^{140}Xe + ^{10}Be, ^{104}Zr + ^{138}Xe + ^{10}Be, and ^{106}Mo + ^{136}Te + ^{10}Be. However, for the fragmentation channels ^{108}Mo + ^{134}Te + ^{10}Be, ^{110}Ru + ^{132}Sn + ^{10}Be, and ^{112}Ru + ^{130}Sn + ^{10}Be, our result differ by three orders of magnitude from the experimental data due to the presence of closed-shell effects ($Z = 50$ and/or $N = 82$). For other fragmentation channels, our results have two orders of magnitude variation.

Due to the excitation energy, the fission fragment can emit several neutrons after fission. In Fig. 5, we also present a comparison of our calculated neutron emission (open circles) from the excited fragments in the ^{10}Be-accompanied spontaneous ternary fission of ^{252}Cf with the available experimental data (solid circles). Here, the results are calculated

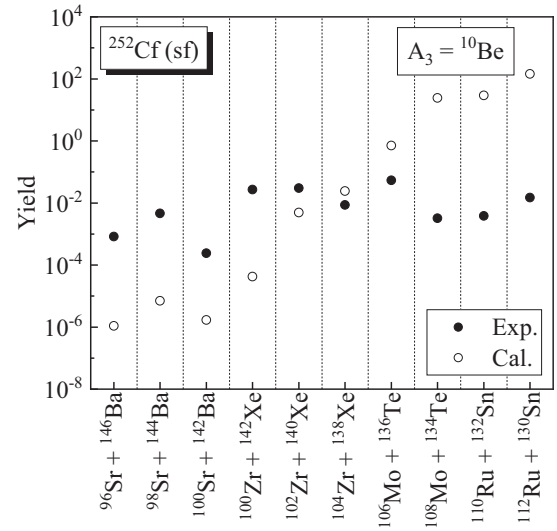

FIG. 4. The calculated ternary fragmentation yields for the ^{10}Be accompanied spontaneous ternary fission of ^{252}Cf are compared with the experimental data of the observed fragments. The experimental data [53] and the calculated results are presented by solid and open circles, respectively.

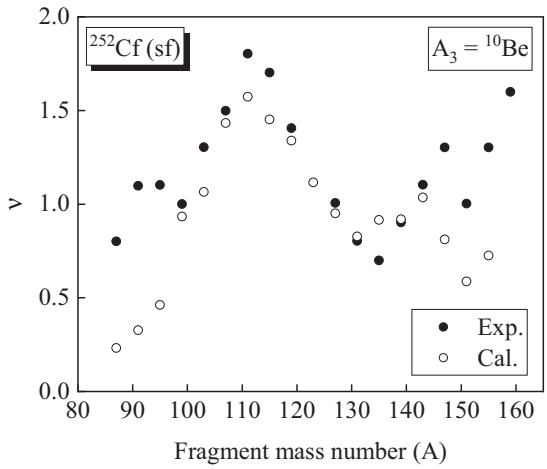

FIG. 5. Neutron emission from individual fragments in the ^{10}Be-accompanied spontaneous fission of ^{252}Cf as a function of the fragment mass number. The experimental data and the calculated results are presented by solid and open circles, respectively.

for spherical fragments only and the presented experimental data are retrieved from Fig. 9 of Ref. [12]. From Fig. 5, it is seen that our calculated results for $\nu(A)$ are comparable with the experimental data, except for some fragment cases. Furthermore, our results overestimate the experimental data for the fragments mass number around 130–140 because it has larger excitation energies due to the closed-shell effects. It is to be mentioned that our calculated neutron emission results also have a saw-tooth structure that is similar to that of the experiment.

IV. SUMMARY AND CONCLUSIONS

In this study, the complete energy and/or T-dependent potential-energy surface for the ternary fragmentation of ^{252}Cf have been analyzed at four different excitation energies of the fissioning parent nucleus, such as $\xi_f^* = 0$ MeV (for spontaneous fission), 6.17 MeV (for thermal-neutron-induced fission), 25 MeV, and 50 MeV. Since the binding energies and the total interaction potential are dependent on the excitation energy and/or temperature, we have calculated the total excitation energy of each ternary fragmentation by using an iterative process. We have presented our results for both the spherical and the deformed ternary fragments as well. From the TF-PES results with the use of T-dependent shell correction energies, we have obtained the highest energy maximum around $Z_3 = 2$–4 with $Z_2 = 40$–48 and $Z_1 = 48$–54 region due to the closed-shell effects of the doubly magic numbers of nuclei. This energy maximum extends further with the increase in ξ_f^*. Besides, some other energy maxima are also obtained around magic and/or semimagic numbers of nuclei. Furthermore, a ternary fragment combination with a heavier third fragment can appear with reasonable probability at a high excitation energy of the fissioning parent nuclei; in particular, the appearance of TTF is found for $\xi_f^* \geqslant 25$ MeV because the heavier third fragments have larger potential V than its ternary reaction Q value. In other words, the total excitation energy of the ternary system with heavier third fragments is $E^* < 0$, for $\xi_f^* < 25$ MeV. To emit these heavier third fragments, the high excitation energy of the fissioning nucleus may be needed.

We have also studied the effect of deformations and its T dependence on the ternary-fragmentation excitation energies of ^{252}Cf. Here, the shell correction energies are made deformation dependent as well as the T dependence. From the TF-PES results of deformed ternary fragments, we have obtained the energy maximum around $Z_3 = 16$ with $Z_2 = 38$–34 and $Z_1 = 44$–48 region due to the presence of higher β_2 deformation values. In addition, a strong maximum is also obtained around $Z_3 = 2$–4 with $Z_1 = 48$–52 and it starts extending with the increase of ξ_f^*. Due to the variation of T_ℓ for each ternary fragmentation, the vanishing of shell structures and deformations at higher excitation energies are not noticeable.

Furthermore, we have also studied the ternary fragmentation yields and neutron emission from the excited fragments in the ^{10}Be-accompanied spontaneous ternary fission of ^{252}Cf and the results are compared with the available experimental data. Due to the closed-shell effects, our calculated yields are larger than the experimental data for fragments with $Z = 50$ and/or $N = 82$. For the neutron emission, a similar trend of experimental data is also predicted from our results.

ACKNOWLEDGMENTS

This work is supported by the National Key Research and Development Program of China under Grants No. 2018YFA0404403 and No. 2016YFE0129300; the National Natural Science Foundation of China under Grants No. 11975167, No. 11761161001, No. 11535004, and No. 11881240623; and the Science and Technology Development Fund of Macau under Grant No. 008/2017/AFJ.

[1] O. Hahn and F. Strassman, Naturwissenschaften **27**, 11 (1939).
[2] Yu. V. Pyatkov, D. V. Kamanin, W. von Oertzen, A. A. Alexandrov, I. A. Alexandrova, O. V. Falomkina, N. A. Kondratjev, Yu. N. Kopatch, E. A. Kuznetsova, Yu. E. Lavrova, A. N. Tyukavkin, W. Trzaska, and V. E. Zhuhcko, Eur. Phys. J. A **45**, 29 (2010).
[3] Yu. V. Pyatkov, D. V. Kamanin, W. von Oertzen, A. A. Alexandrov, I. A. Alexandrova, O. V. Falomkina, N. Jacobs, N. A. Kondratjev, E. A. Kuznetsova, Yu. E. Lavrova, V. Malaza, Yu. V. Ryabov, O. V. Strekalovsky, A. N. Tyukavkin, and V. E. Zhuchko, Eur. Phys. J. A **48**, 94 (2012).
[4] H. Diehl and W. Greiner, Nucl. Phys. A **229**, 29 (1974).
[5] D. N. Poenaru, R. A. Gherghescu, and W. Greiner, Nucl. Phys. A **747**, 182 (2005).
[6] K. Manimaran and M. Balasubramaniam, Phys. Rev. C **83**, 034609 (2011).
[7] J. P. Lestone, Phys. Rev. C **70**, 021601(R) (2004).
[8] J. P. Lestone, Int. J. Mod. Phys. E **17**, 323 (2008).

[9] P. Fong, Phys. Rev. C **3**, 2025 (1971).
[10] I. Halpern, in *Proceedings of the Second IAEA Symposium on Physics and Chemistry of Fission, Salzburg 1965* (International Atomic Energy Agency, Vienna, 1965), Vol. 2, p. 369.
[11] U. Köster, H. Faust, G. Fioni, T. Friedrichs, M. Groß, and S. Oberstedt, Nucl. Phys. A **652**, 371 (1999).
[12] A. V. Andreev, G. G. Adamian, N. V. Antonenko, S. P. Ivanova, S. N. Kuklin, and W. Scheid, Eur. Phys. J. A **30**, 579 (2006).
[13] R. B. Tashkhodjaev, A. K. Nasirov, and W. Scheid, Eur. Phys. J. A **47**, 136 (2011).
[14] A. K. Nasirov, W. von Oertzen, A. I. Muminov, and R. B. Tashkhodjaev, Phys. Scr. **89**, 054022 (2014).
[15] W. von Oertzen and A. K. Nasirov, Phys. Lett. B **734**, 234 (2014).
[16] R. B. Tashkhodjaev, A. I. Muminov, A. K. Nasirov, W. von Oertzen, and Yongseok Oh, Phys. Rev. C **91**, 054612 (2015).
[17] V. I. Zagrebaev and W. Greiner, Int. J. Mod. Phys. E **17**, 2199 (2008).
[18] V. I. Zagrebaev, A. V. Karpov, and W. Greiner, Phys. Rev. C **81**, 044608 (2010).
[19] A. V. Karpov, Phys. Rev. C **94**, 064615 (2016).
[20] V. Yu. Denisov, N. A. Pilipenko, and I. Yu. Sedykh, Phys. Rev. C **95**, 014605 (2017).
[21] I. Tsekhanovich, Z. Büyükmumcu, M. Davi, H. O. Denschlag, F. Gönnenwein, and S. F. Boulyga, Phys. Rev. C **67**, 034610 (2003).
[22] K. Manimaran and M. Balasubramaniam, Phys. Rev. C **79**, 024610 (2009).
[23] K. Manimaran and M. Balasubramaniam, J. Phys. G **37**, 045104 (2010).
[24] K. Manimaran and M. Balasubramaniam, Eur. Phys. J. A **45**, 293 (2010).
[25] K. R. Vijayaraghavan, M. Balasubramaniam, and W. von Oertzen, Phys. Rev. C **90**, 024601 (2014).
[26] K. R. Vijayaraghavan, M. Balasubramaniam, and W. von Oertzen, Phys. Rev. C **91**, 044616 (2015).
[27] M. Balasubramaniam, K. R. Vijayaraghavan, and K. Manimaran, Phys. Rev. C **93**, 014601 (2016).
[28] K. P. Santhosh, S. Krishnan, and B. Priyanka, J. Phys. G **41**, 105108 (2014).
[29] K. P. Santhosh, S. Krishnan, and B. Priyanka, Phys. Rev. C **91**, 044603 (2015).
[30] K. P. Santhosh and S. Krishnan, Eur. Phys. J. A **52**, 108 (2016).
[31] M. Balasubramaniam, C. Karthikraj, S. Selvaraj, and N. Arunachalam, Phys. Rev. C **90**, 054611 (2014).
[32] C. Karthikraj and Z. Ren, J. Phys. G **44**, 065102 (2017).
[33] H. J. Krappe, Phys. Rev. C **59**, 2640 (1999).
[34] M. Wang, G. Audi, F. G. Kondev, W. J. Huang, S. Naimi, and X. Xu, Chin. Phys. C **41**, 030003 (2017).
[35] C. Karthikraj and Z. Ren, Phys. Rev. C **96**, 064611 (2017).
[36] C. Karthikraj, N. S. Rajeswari, and M. Balasubramaniam, Phys. Rev. C **86**, 014613 (2012).
[37] C. Karthikraj and M. Balasubramaniam, Phys. Rev. C **87**, 024608 (2013).
[38] W. Myers and W. J. Swiatecki, Nucl. Phys. **81**, 1 (1966).
[39] G. Audi, A. H. Wapstra, and C. Thibault, Nucl. Phys. A **729**, 337 (2003).
[40] P. Möller, A. J. Sierk, T. Ichikawa, and H. Sagawa, At. Data Nucl. Data Tables **109**, 1 (2016).
[41] G. Sawhney, R. Kumar, and M. K. Sharma, Phys. Rev. C **86**, 034613 (2012).
[42] M. Rashdan, A. Faessler, and W. Wadia, J. Phys. G **17**, 1401 (1991).
[43] M. Münchow and W. Scheid, Nucl. Phys. A **468**, 59 (1987).
[44] V. Yu. Denisov, Phys. Rev. C **91**, 024603 (2015).
[45] V. Yu. Denisov and N. A. Pilipenko, Phys. Rev. C **76**, 014602 (2007).
[46] V. Yu. Denisov, T. O. Margitych, and I. Yu. Sedykh, Nucl. Phys. A **958**, 101 (2017).
[47] A. Bohr and B. Mottelson, in *Nuclear Structure* (W. A. Benjamin Inc., New York, Amsterdam, 1974), Vol. II.
[48] S. Hilaire, Phys. Lett. B **583**, 264 (2004).
[49] O. A. P. Tavares and E. L. Medeiros, J. Phys. G **30**, 395 (2004).
[50] A. V. Andreev, G. G. Adamian, N. V. Antonenko, S. P. Ivanova, and W. Scheid, Eur. Phys. J. A **22**, 51 (2004).
[51] R. K. Gupta, in *Clusters in Nuclei*, Lecture Notes in Physics Vol. 818, edited by C. Beck (Springer, Berlin, Heidelberg, 2010), Vol. 1, pp. 223–265, http://doi.org/10.1007/978-3-642-13899-7_6.
[52] M. T. Senthil Kannan and M. Balasubramaniam, Eur. Phys. J. A **53**, 164 (2017).
[53] J. H. Hamilton *et al.*, Prog. Part. Nucl. Phys. **38**, 273 (1997).
[54] A. Sandulescu, F. Cârstoiu, S. Misicu, A. Florescu, A. V. Ramayya, J. H. Hamilton, and W. Greiner, J. Phys. G **24**, 181 (1998).